Article

Composites of Biopolymers and ZnO NPs for Controlled Release of Zinc in Agricultural Soils and Timed Delivery for Maize

Natercia C. T. Martins, Astrid Avellan, Sandra Rodrigues, Diana Salvador, Sónia Morais Rodrigues, and Tito Trindade

ACS Appl. Nano Mater., **Just Accepted Manuscript** • Publication Date (Web): 30 Jan 2020

Composites of Biopolymers and ZnO NPs for Controlled Release of Zinc in Agricultural Soils and Timed Delivery for Maize

Natércia C.T. Martins [a,b*], Astrid Avellan[a], Sandra Rodrigues[a], Diana Salvador[a], Sónia M. Rodrigues[a], Tito Trindade[b]

[a] CESAM & Department of Chemistry, University of Aveiro, Campus Universitário de Santiago, 3810-193 Aveiro, Portugal
[b]CICECO & Department of Chemistry, University of Aveiro, Campus Universitário de Santiago, 3810-193 Aveiro, Portugal

ABSTRACT

Zinc deficiency is a widespread micronutrient deficiency problem affecting crops worldwide. Unlike conventional ionic fertilizers (Zn as salt or chelated forms), Zn-based engineered nanomaterials (ENMs) have the potential to release Zn in a controlled manner, reducing Zn losses through leaching upon application to soil. In this work, composites made of biopolymers (microcrystalline cellulose, chitosan and alginate) and ZnO nanoparticles (4-65% Zn w/w) were prepared. Their potential for Zn controlled release was tested in four agricultural soils of distinct pH and organic matter content over 30 days. While conventionally used Zn salts leached from the soil resulting in very low $CaCl_2$-extractable Zn concentration, Zn in ZnO NPs was less labile, and ZnO-biopolymers maintained a better constant supply of $CaCl_2$-extractable Zn than all other treatments. ZnO NPs/alginate beads prepared by crosslinking with $CaCl_2$ presented the slowest Zn release kinetics.

As assessed with maize plants grown in poor Zn acidic soil (LUFA 2.1, pH=5.2), this constant Zn release from ZnO NPs/alginate beads resulted in a steadier Zn concentration in the soil pore water over time. These results further indicate that ZnO NPs/alginate beads could meet the maize Zn needs while avoiding the early stage Zn toxicity induced by conventional Zn supplies, demonstrating that these ENMs are a sustainable way to supply Zn in a controlled manner in acidic soils. The impact of plant exudates on Zn bioavailability in the soil under maize-root influence (rhizosphere) is also discussed, underlying the need to study the fate of micronutrients in the rhizosphere to better predict its long-term bioavailability in bulk soils.

KEYWORDS: controlled release, micronutrients, biopolymers, composites, zinc oxide nanoparticles, maize rhizosphere

* Corresponding author. Tel.: +351 234 401 405; fax: +351 234 370 084.
E-mail address: natercia@ua.pt (Natércia C.T. Martins)

1. INTRODUCTION

In the last decades, nanotechnology has achieved great progress and it has been applied with success in several fields such as electronics, energy, environmental science and medicine.[1–4] Nanotechnology applications in agriculture are increasing and need further exploration.[5] Indeed, there are already some examples in the literature that show the potential of nanomaterials in improving agrochemical delivery, seed germination, plant growth and protection, pathogen detection and pesticide residue detection.[6–12]

Recently, nanomaterials were used in agricultural production to mitigate environmental problems caused by conventional intensive application of fertilizers.[13,14] Due to a lack of synchronization between the release of minerals from bulk ionic fertilizers and uptake by plants, only a small part of the fertilizers applied to the soils are actually used by plants (30-50 %).[15] The remaining Zn applied forms nonbioavailable complexes in soils or it is removed by leaching or run-off causing negative environmental impacts.[15–17] Using nanomaterials to apply essential micro and macro nutrients to plants is a promising fertilization method.[18] Nanomaterials can be used to control the release of nutrients in soil-plant systems according to specific soil biochemical conditions, plant species and plant life cycle stages, allowing a reduction of nutrients loss and of fertilizers application rates. [16,19]

Essential plant nutrients include nitrogen, phosphate, potassium, calcium (macronutrients) iron, zinc and copper (micronutrients). Zn is crucial for plant growth and development as it takes part in a wide range of plant biochemical processes. Zinc plays a vital role in chlorophyll synthesis, in regulation of plant growth hormones, in maintaining healthy root systems, in activating enzymes and detoxifying free radicals, and in preserving tolerance to plant stressors.[18,20] This element is also a very important nutrient for human health. In developing countries, where staple diets are plant-based, Zn deficiency is associated with growth retardation, impaired brain development and increased susceptibility to infectious diseases such as pneumonia and diarrhea.[21]

Wheat, rice and maize, are strategic crop plants for human nutrition and very sensitive to Zn deficiencies in soils.[22] To grow without developing signs of Zn deficiencies, gramineous plants, and maize in particular, usually need around 1mg of extractable Zn per Kg of soil,[23] or 50 µg of Zn per L of soil pore water.[14] This bioavailable zinc concentrations will depend on the soil pH, oxide species and organic matter content.[24,25]

Zinc deficiency is a common problem in soils worldwide.[26] To correct Zn deficiency and prevent losses on crops, fertilizers containing Zn are added to the soils. Water soluble salts such as $ZnSO_4$ or $ZnCl_2$ are often used as Zn fertilizers.[27,28] These salts are a source of Zn readily

available for plants; however, these nutrients can be easily lost by leaching and run-off from soils, particularly in acidic soils under heavy rainfall or intensive watering. ZnO in bulk or nanoparticles (NP) form can be an alternative to the use of ionic Zn forms as fertilizers. The effects of ZnO NPs on soils and crops has been recently subject of debate. There are a few papers reporting phytotoxicity of ZnO NPs; however, in the majority of these studies the experiments were designed using very high doses of ZnO NPs (higher than those used in conventional fertilization) and very short exposure times.[29,30] In fact, there are also many studies that show that at low doses ZnO NPs are beneficial to crops.[14,16,31] Moreover, a recent study[32] demonstrated that in acidic soils, due to rapid dissolution of ZnO NPs, the risks of using ZnO NPs as fertilizer are not different from those of using ionic Zn.

ZnO NPs dissolve relatively fast in acidic soils and can also be subject to aggregation leading to low Zn availability to crops and significant Zn losses by soil leaching and wash-off which result in Zn contamination of surface and groundwater.[13,32] We hypothesise that the immobilization of ZnO NPs onto polymeric substrates to form composites that release Zn in a slower and controlled manner can be a solution to these problems.

Biopolymers such as cellulose, alginate or chitosan can be interesting choices to be used as substrates for immobilization of nanoparticles to produce composite fertilizers because these are natural, low cost and biodegradable polymers.[33] Moreover, some of these polymers are themselves beneficial to plants. This is the case of chitosan which is known to act as promoter of plant growth and as an activator of plant defense system.[34] There are reports in literature concerning the use of biopolymers for controlled release of nutrients; however, the majority of the research is directed to macronutrients and the release tests are mainly done in water.[35–37] Soil is a very complex matrix and the nature and composition of the soil have a significant impact on the behaviour and fate of the materials, particularly on dissolution. Tests of release of nutrients from polymer-based materials in realistic soil conditions are therefore most needed.

In this work, a series of composites of biopolymers and ZnO NPs were prepared (by the methods shown in Scheme 1), their potential as materials for the controlled release of Zn in agricultural soils was tested, and their impact towards maize plant was assessed. The materials were added to soils with distinct pH and organic matter content. A screening soil incubation study (7 days) was performed to determine the amount of labile Zn dissolved from the different ZnO NPs composites along time in different agricultural soils, using a soil 0.01 M $CaCl_2$ extraction.[38] The rate of Zn release was correlated with the type of polymeric matrix, method of preparation of the materials and characteristics of the soils. The extractability of Zn from the most promising material, ZnONPs/alginate beads, was further studied in an experiment with a

soil incubation period of 30 days to evaluate the potential of this material to be used for controlled release of Zn in agricultural soils. Finally, the ability of ZnO NPs/alginate beads to supply Zn to maize plants was tested in soil LUFA 2.1, in comparison to ZnO NPs and $ZnCl_2$ for 30 days. We hypothesised that this material can potentially be used to control the effectivity of the application of Zn fertilizer in soil and thus reduce environmental collateral damages of Zn loss upon soil application.

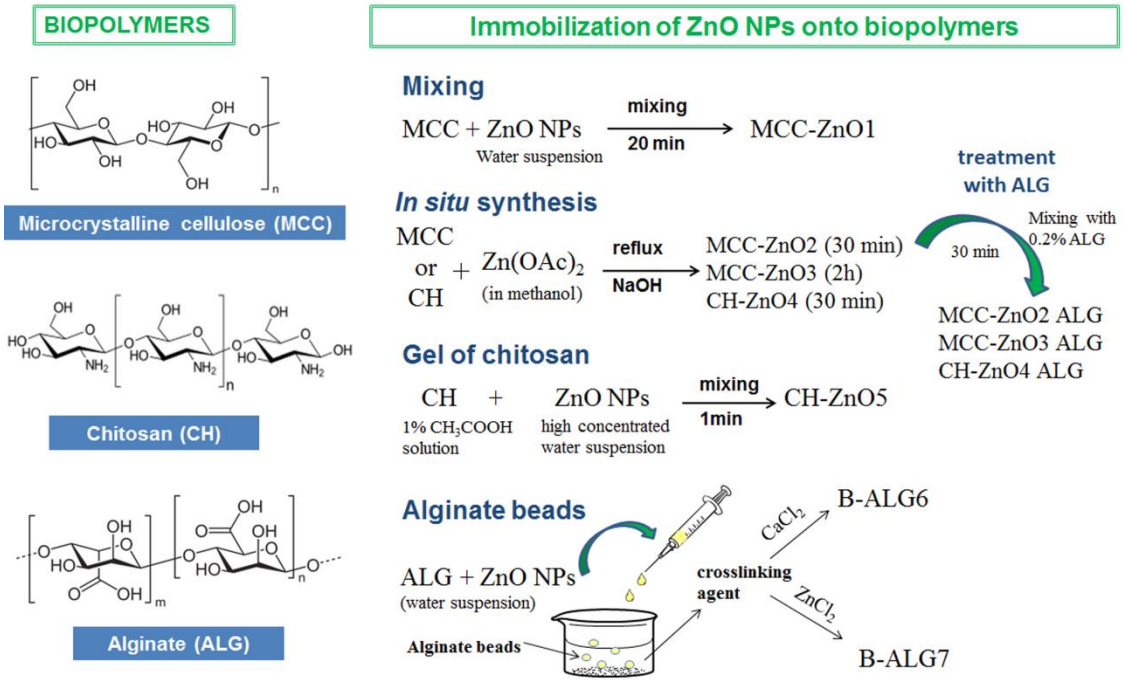

Scheme 1 Methods used for the preparation of the composites prepared in this work

2. EXPERIMENTAL SECTION

2.1 Materials and analytical methods

Microcrystalline cellulose (MCC), chitosan (CH) (low molecular weight, degree of deacetylation 75-85%) and alginic acid sodium salt from brown algae (ALG) were purchased from Sigma-Aldrich and were used as received. Calcium chloride (>99%, ACS grade), Zinc chloride (>98%, ACS grade) and zinc acetate dihydrate (>98%) were obtained by Merck. Commercial ZnO NPs were purchased from Nanostructure & Amorphous Materials Inc., USA (99.5% purity, 20 nm diameter size as reported by the manufacturer).

Four soils were used in this study: standard agricultural soils LUFA 2.1 and LUFA 2.2 were purchased from LUFA Speyer in Germany; two agricultural calcareous soils were collected in

south Portugal (soil codes: "DE" and "VV"; soils were collected at the 0-20 cm layer, using plastic spades and transported to the laboratory for pre-treatment and analysis). The LUFA soils were included because they are commonly used in metal bioavailability studies and therefore would be easier to compare our results with other found in literature. Soil characterization was performed on the <2 mm air-dried soil fraction. The pH of samples was measured using a glass electrode in a 1:5 (v/v) suspension of ashes/soils in $CaCl_2$ (according to ISO 10390:1994). A laser diffraction particle size analyser (Coulter LS230) was used to determine clay, silt and sand content for ashes and soils (limit of detection = 0.040 µm). Organic carbon (OrgC) in soils was determined after addition of hydrochloric acid to re-move carbonates (ISO 10694:1995). The water holding capacity (WHC) was determined by saturating the air-dried soils in a cylinder during 24 hours. The cylinder was then placed on an absorbent membrane until the excess water was drawn away by gravity. Once equilibrium was reached (24-48 hours), the WHC was calculated based on the weight of the water held in the sample vs. the sample dry weight. The pseudo-total content of Zn in soils was determined by aqua regia (AR) digestion (according to ISO 11466:1995) and analysis by ICP-MS (Agilent 7700). Soil extractable Zn was determined by extraction with 0.01 M $CaCl_2$ (1:10 weight:volume ratio) and analysis by ICP-MS. Samples for analysis by ICP-MS were acidified with 20% HNO_3 (final HNO_3 concentration, 1%) kept at 4º C and analyzed within 1–4 days after collection. Instrument calibration standards were prepared in the same acid matrix as the soil extracts and spike recovery samples were included in all analyses. Before analysing by ICP-MS, the samples were diluted in ultra-pure water (1:10 v/v). The detection limit for this Zn analysis was (8 µg/L). All analysis were performed in triplicate.

LUFA 2.1 is a loamy sand soil containing 3 wt % clay, 11 wt % silt, and 86 wt % sand. It has an organic carbon content of 0.71 ± 0.08%, a pH (0.01M $CaCl_2$) of 5.2 and maximum water holding capacity of 32%. LUFA 2.2. is a sandy loam soil containing 8 wt % clay, 15.8 wt % silt, and 76.2 wt % sand. It has an organic carbon content of 1.61 ± 0.15% and a pH (0.01M $CaCl_2$) of 6.1 and maximum water holding capacity of 43%. Moreover, these soils have a low content of extractable Zn (0.86 mg/kg for LUFA 2.1 and 0.26 mg/kg for LUFA 2.2, $CaCl_2$ extraction) making background interference minimal.

Soil DE has an organic carbon content of 7.2%, a pH (0.01M $CaCl_2$) of 7.0, a maximum water holding capacity of 48% and it contains 0.1 wt % clay. Soil VV has an organic carbon content of 0.9%, a pH (0.01M $CaCl_2$) of 6.9, a maximum water holding capacity of 27% and contains 10.4 wt % clay. The concentration of extractable Zn in soils DE and VV was under the detection limit of ICP-MS (8 µg/L).

All the dry soils (without zinc amendments) were sterilized by autoclaving (121°C) 1h prior to use in the incubation tests.

All chemicals were of analytical grade or better and all solutions were prepared using ultra-pure water (MilliQ water).

2.2 Preparation of nanocomposites

Table 1 presents the list of the composites prepared in this work along with the method used for their synthesis and the respective Zn content (as determined by atomic absorption spectroscopy following digestion). The next sections present a detail description of the methods of preparation of the composites.

2.2.1 Composite obtained by mixing MCC with ZnO NPs

Commercial ZnO NPs (0.018 g) were dispersed in 50 ml of Milli-Q water and the resulting suspension was sonicated using an ultrasonic bath for 5 min. The suspension was placed under magnetic stirring and then 0.2 g of MCC were added. After 20 min of mixing, the resulting nanocomposite (identified as MCC-ZnO1) was collected by filtration, thoroughly washed with distilled water and dried under vacuum in a desiccator with silica gel overnight.

2.2.2 *In situ* synthesis of ZnO NP on biopolymers

ZnO NPs were grown at polymers surfaces (MCC or CH) by zinc acetate hydrolysis with NaOH in alcoholic medium in the presence of water. The method used was an adaptation of the procedure described by Wu et al.[39] for the synthesis of ZnO NPs. In the present study the reaction was performed in the presence of the biopolymers. In this preparation, 0.5g of biopolymer were mixed with 40 ml of a methanolic solution of $Zn(OAc)_2.2H_2O$ (3.8×10^{-2} M) at room temperature during 1 hour. The suspension was then refluxed for 45 min under stirring and 10 ml of water were added followed by dropwise addition of 30 ml of NaOH methanolic solution (0.1 M). After 30 minutes or 2 hours of reflux the reaction was stopped, and the suspension was allowed to cool to room temperature. The final composites were isolated by filtration, washed two times with 10 ml of ethanol and dried overnight under vacuum in a desiccator with silica gel. This procedure generated the composites here identified as MCC-ZnO2 (30 min reaction), MCC-ZnO3 (2h reaction) and CH-ZnO4 (30 min reaction).

Table1

List of all composites prepared

Sample	Matrix	Method	ZnO NPs diameter [a] (nm)	Zn [c] (% w/w)	Deposition efficiency (%)
MCC-ZnO1	MCC	Mixing MCC with ZnO NPs	87 ± 24[b]	3.6 ± 0.6	54[d]
MCC-ZnO2	MCC	In situ synthesis of ZnO NPs, 30 min of reaction	129 ± 39	13.5 ± 2.6	85[e]
MCC-ZnO2 ALG	MCC	Treatment of MCC-ZnO2 with alginate	129 ± 39	12.9 ± 2.5	----
MCC-ZnO3	MCC	In situ synthesis of ZnO NPs, 2h of reaction	120-400	15.1 ± 1.8	94[e]
MCC-ZnO3 ALG	MCC	Treatment of MCC-ZnO3 with alginate	120-400	13.2 ± 1.5	-----
CH-ZnO4	CH	In situ synthesis of ZnO NPs, 30 min of reaction	113 ± 33	12.9 ± 1.6	81[e]
G-CH-ZnO5	CH	Gel of chitosan and ZnO NPs	87 ± 24[b]	64.6 ± 7.0	87[d]
B-ALG6	ALG	ZnO NPs/alginate beads Crosslinking with $CaCl_2$	87 ± 24[b]	11.8 ± 1.1	88[d]
B-ALG7	ALG	ZnO NPs/alginate beads Crosslinking with $ZnCl_2$	87 ± 24[b]	33.5 ± 3.5	> 100[d]

[a] based on SEM images of at least 150 particles (results are presented as mean ± standard deviation or size range); Only two composites (MCC-ZnO3 and MCC-ZnO3 ALG) exhibited significantly higher diameter ($p < 0.05$) than the remaining ones.; [b] commercial nanoparticles; [c] results are presented as mean ± standard deviation (3 replicates of each material); [d] deposition efficiency = ratio between the mean mass of Zn measured in the composite and the mass of Zn in the suspension of ZnO NPs; [e] deposition efficiency = ratio between the mean mass of Zn measured in the composite and the expected mass of Zn (considering a yield of 100% in the *in situ* synthesis of ZnO NPs).

2.2.3 Alginate treated MCC-ZnO nanocomposites

Composites MCC-ZnO2 and MCC-ZnO3, obtained by *in situ* synthesis, were further treated with a solution of alginate. Typically, 0.2 g of MCC-ZnO2 or MCC-ZnO3 composites were treated with 50 ml of a solution containing 0.2 g of sodium alginate with stirring for 1 hour.

The resultant composites, identified as MCC-ZnO2 ALG and MCC-ZnO3 ALG, were then isolated by filtration, thoroughly washed with distilled water and dried under vacuum in a desiccator with silica gel overnight.

2.2.4 Gel of chitosan and ZnO NPs

A gel of chitosan and ZnO NPs was prepared by the adaptation of the method reported by Vasile et al.[40]. Chitosan (0.025 g) was dissolved in 10 ml of acetic acid solution (1%). Commercial ZnO NPs (0.3 g) were suspended in 5 ml of distilled water and sonicated using an ultrasonic bath for 5 min. The suspension was quickly added to a 10 ml solution of chitosan (0.025 g) in acetic acid (1%) under magnetic stirring. In a few seconds a ZnO-chitosan gel was formed. The gel with a consistency of a gelatine pudding was removed from beaker and cut in pieces that were dried at room temperature. The resulting films were ground in a mortar to obtain a powder (G-CHZnO5).

2.2.5 Alginate beads containing ZnO NPs

Sodium alginate (0.75 g) was stirred in 50 ml distilled water for 1 hour to ensure the formation of a homogeneous solution. ZnO NPs (0.150 g) were then added to the alginate solution and the mixture was left under continuous stirring. The milky mixture was transferred to a syringe and added drop by drop into a beaker containing 100 ml of 0.25 M solution of the crosslinking agent ($CaCl_2$ or $ZnCl_2$) under moderate stirring. The resulting alginate beads were allowed to stay for 30 min in the crosslinking agent solution and then were separated by filtration, thoroughly washed with distilled water and dried at 30 °C for one day. For soil tests the beads were ground in a mortar to obtain a powder. By this method, composites B-ALG6 (crosslinking with $CaCl_2$) and B-ALG7 (crosslinking with $ZnCl_2$) were obtained.

2.3 Materials characterization

Scanning electron microscopy (SEM) images were obtained with a Hitachi S4100 or a Hitachi SU-70 instrument fitted with an energy dispersive spectroscopy (EDS) accessory (EDSdetector: Bruker AXS; software: Quantax). Samples were deposited on carbon tape and coated with carbon before SEM analysis. Transmission electron microscopy (TEM) was

performed with a Hitachi H-9000 or a JEOL 2200FS electron microscope equipped with Oxford Energy Dispersive X-rays (EDS) detector and in-column Omega filter, operated at 300 kV. The samples for TEM were prepared by depositing a drop of a diluted suspension of the materials in ultra-pure water onto the surface of an Agar Scientific carbon-coated copper grid and then allowing the solvent to evaporate. To calculate the mean size of ZnO NPs based on SEM or TEM images at least 150 particles were measured.

The total Zn concentration in the composite materials was evaluated by atomic absorption spectroscopy (AAS) using a Thermo Scientific ICE 3000 series AA spectrometer (detection limit: 50 µg/L). Before AAS the samples were submitted to acid digestion with HNO_3 (68%) in a microwave oven. Instrument calibration standards were prepared in the same acid matrix as the soil extracts. All analysis were performed in triplicate.

Zeta potential measurements were performed using a Zeta Sizer Nano Series (Malvern) equipment. The optical spectra were recorded using a Jasco V-560 UV/VIS spectrophotometer; for the solid samples the spectra were recorded in the diffuse reflectance mode using MgO as reference. Powder X-rays Diffraction (XRD) patterns of the solid samples were recorded with a Philips X'Pert instrument operating with Cu-Kα radiation (λ = 1.543178 Å) at 40 kV and 50 mA. FTIR spectra (128 scans at a resolution of 4 cm^{-1}) were collected with a Mattson 7000 spectrometer coupled to a horizontal attenuated total reflectance (ATR) cell.

2.4 Soil amendment and incubation

Soils LUFA 2.1, LUFA 2.2, DE and VV were amended with ZnO NPs, $ZnCl_2$ or biopolymer composites loaded with ZnONPs to obtain a Zn concentration of 100 mg/kg dry soil.

ZnO NPs and ZnO NPs composite powders were dispersed in Milli-Q water (pH=7) and the suspensions were then sonicated in an ultrasonic bath for 2 min. The dispersed nanomaterials were then immediately added to soil. $ZnCl_2$ powder was dissolved in Milli-Q water before being amended to the soil. The amount of Milli-Q water added to each soil was the necessary to ensure that each soil was at 50% of their maximum water holding capacity after amendment.

First, a screening test was done in acid soils LUFA 2.1 and LUFA 2.2 with all the materials for two incubation times 1 and 7 days. Typically, 4 ml or 5.6 ml of $ZnCl_2$ solution or ZnO NPs materials suspensions were added to 25 g of dried LUFA 2.1 or LUFA 2.2 soils respectively. 18 g (dry weight) of each amended soil were then divided into 6 centrifuge tubes (3 replicates, 2 incubation periods) with 3 g of soil each. The soil samples were then incubated under aerobic conditions at room temperature for 1 and 7 days before being extracted. The moisture content

of the soil samples was kept at 50% of their maximum water holding capacity by daily additions of MilliQ water.

The material that presented the lowest Zn release (B-ALG6) was tested in a period of 30 days of incubation in acid soils LUFA 2.1 and LUFA 2.2 and neutral soils (DE and VV) in order to better understand the role of pH on Zn release from this composite. In this case, soil samples were incubated under aerobic conditions at room temperature for 1, 2, 4, 7, 15 and 30 days before being extracted.

2.5 Maize culture in LUFA 2.1 soil amended with different Zn sources

Maize seeds (Zea Mays) were surface sterilized with bleach, thoroughly rinsed with deionized water and germinated on plate with saturated humidity in the dark at 20°C for 5 days. LUFA 2.1 soil (900 g) was amended with different treatments, as described above. Homogenisation of the soil with the different treatments was done by stirring the soil (3 times during 5 minutes) after the addition of the materials suspensions to ensure for a good homogenisation of the treatments. Soils were prepared to reach 50% of the maximum water holding capacity. After homogenisation, the soils of the different treatments were transferred into pots. In the middle of each pot, a filtration device was horizontally placed. These samplers (Rhizon® Flex, 5cm)[41] are made of polyethersulfone membranes of 0.12-0.17 µm nominal pore size, connected to a luer lock through a 30 cm long PVP-PE tubing, that allowed for pore water sampling outside of the pot, without disturbing the soil. These membrane filters are made of inert polymers with no ion exchange properties to minimize sorption. Pore water (4-7 ml) was sampled from each pot 2, 6, 10, 24 and 29 days after the seed transfer. An aliquot was used for pH measurement, and the rest was acidified (2% HNO_3) and stored at 4°C for total Zn measurement by ICP-MS, as described in section 2.1.

A rope made of 100% cotton connecting the soil to a nutritive solution allowed, through capillary exchanges, to maintain the soil humidity constant over time. The nutritive solution used was ¼ strength Hoagland solution,[42] prepared without Zinc micronutrients to ensure that the plant will not undergo other deficiencies than Zn.

Four maize seedlings were transferred per pot of 900 g of soil amended with 30 ppm or 100 ppm (as Zn) of either $ZnCl_2$, ZnO NPs or ZnO NPs/alginate (B-ALG6), or in a control soil (ultrapure water, UP). Alginate controls with similar alginate concentration as the B-ALG6 30 ppm and 100 ppm treatments were also run. These resulted in 9 treatments and four maize plants per treatments, namely water, ALG 30eq, ALG 100eq, $ZnCl_2$ 30 ppm, $ZnCl_2$ 100 ppm, ZnO 30

ppm, ZnO 100 ppm, B-ALG6 30 ppm, B-ALG6 100 ppm. The plants were then grown under Tubo T8 G13 58W 5000LM 6500K fluorescence lamps under a 16:8 light:night photoperiod over 29 days.

At the end of the experiment, all the plants were collected. Shoots were separated from the root system and pictures were taken. Shoots and roots were dried at 60°C during 48 h to assess for dry biomass. Length of the leaves was measured on the plant pictures using the ImageJ software. Shoot density was calculated as a ratio of the biomass divided by the total leaves length of each plant.

Bulk soil was separated from the rhizosphere soil following previous established procedures,[43] dried at 60°C until the dry mass didn't change and used for $CaCl_2$ extraction as described below for pH measurements and Zn concentration measurements.

2.6 Extraction test to determine the extractable pool of Zn in amended soil

After 1, 2, 4, 7, 15 or 30 days of incubation without plants, and 30 days of incubation with plants, dry soil samples of soil LUFA 2.1, LUFA 2.2, DE and VV amended with ZnO NPs, $ZnCl_2$ or biopolymer composites loaded with ZnONPs were extracted in triplicate with a 1:10 soil:$CaCl_2$ ratio using a 0.01 M $CaCl_2$ solution in centrifuge tubes. Centrifuge tubes were laid horizontally and shaken for 2 hours, using a reciprocal shaker at 180 rpm. After extraction, all samples were centrifuged at 1022 g for 10 min, and the supernatants were filtered using a 0.2 µm PTFE syringe filter. It should be noticed that at first supernatants were filtered with 0.2 µm and 3kDa filters and it was observed that Zn content of the extracts were similar in the two cases. Therefore, in the following experiments only 0.2 µm filters were used. Soil blanks (no Zn treatment, only ultra-pure water added to ensure the same moisture content) were used as controls. The pH values of $CaCl_2$ extracts were measured. After that, all extracts were acidified with a 20% solution of HNO_3 (final HNO_3 concentration of 2%) and analyzed for Zn concentration by ICP-MS, as described in Section 2.1.

2.7 Statistical analysis

The software SPSS 24.0 by IBM for MacOS was used for calculation of descriptive statistics and for statistical analysis of data. For the experiment without maize, comparison of results for different materials and respective Zn release in soil was based on analysis of variance (ANOVA) provided by the General Linear Model (univariate analysis). Bonferroni post hoc

tests were applied to explore differences between group means. To compare plant biomass and density, ANOVA was done using a Tukey test.

3. RESULTS AND DISCUSSION

3.1 Materials characterization

SEM analysis of commercial ZnO NPs powders showed that the particles were nearly spheroidal with mean diameter of 87 ± 24 nm (Fig. S1, supporting information). TEM analysis of a diluted suspension of ZnO NPs in water was also performed (Fig. S2, supporting information). The diameter of the nanoparticles calculated from TEM images was in good agreement with the obtained by SEM, which also showed that the ZnO NPs did not aggregate in water (at least in the time of preparation of the suspension: 5 min). The size distribution of ZnO NPs calculated from SEM and TEM images was higher than that reported by the manufacturer (20 nm). This discrepancy could be attributed to some aggregation of metal oxide nanoparticles or to low accuracy of the size values reported.[44] Zeta (ζ) potential measurements of a 200 mg L^{-1} ZnO NPs suspension showed that the nanoparticles are positively charged (+ 22.1 ± 0.379 mV at pH 7.2). Powder XRD pattern of ZnO NPs (Fig. S3, supporting information) presents the characteristic peaks of *wurtzite* crystal structure (JCPDF Nº 36-1451). The UV-Vis reflectance spectrum of ZnO NPs showed the characteristic absorption edge associated to the energy gap of ZnO, with maximum of absorption at 360 nm (Fig. S4, supporting information). The absorption maximum of ZnO NPs was blue shifted relative to bulk ZnO (380 nm) due to the quantum confinement effect of the ZnO nanostructure.[45]

Several composites of biopolymers (microcrystalline cellulose, chitosan and alginate) and ZnO NPs were produced using different methodologies (Table 1, experimental section).

The MCC-ZnO1 composite was prepared by mixing MCC with the commercial nanoparticles. The efficiency of the deposition of ZnO NPs on MCC fibers was low (54%) and the Zn content on the final composite was only 3.6 % (w/w). The low deposition efficiency could be related with the fact that positively charged ZnO NPs can only bind to the negatively charged MCC fibers (zeta potential of -18.6 mV at pH 7.2) by weak electrostatic forces. SEM (Fig.1), EDS (Fig. S5, supporting information) and XRD (Fig. S6, supporting information) analysis of MCC-ZnO1 sample confirmed the presence of ZnO NPs over MCC fibers; however, the nanoparticles do not fully cover the polymer surface. Moreover, the deposition of the ZnO NPs seems to be non-homogeneous since it is possible to find areas in the matrix with low (Fig.

1a) and high density of nanoparticles (Fig. 1b). Areas with high density of nanoparticles were attributed to the existence of a higher number of carboxyl groups (which have a negative charge) on MCC fibers. XRD of the sample (Fig. S6, supporting information) shows the characteristic Bragg reflections of ZnO (*wurtzite*) (2θ = 31.8º, 34.6º, 36.4º, 47.8º, 56.7º, 63.1º and 68.3º) and of MCC (cellulose I) (2θ = 14.3º, 15.9º, 22.6º). The UV-vis reflectance spectrum of the nanocomposite showed the presence of the absorption edge associated to the energy gap of ZnO, with an onset of absorption close to that observed in the spectrum of commercial ZnO NPs (Fig. S4, supporting information).

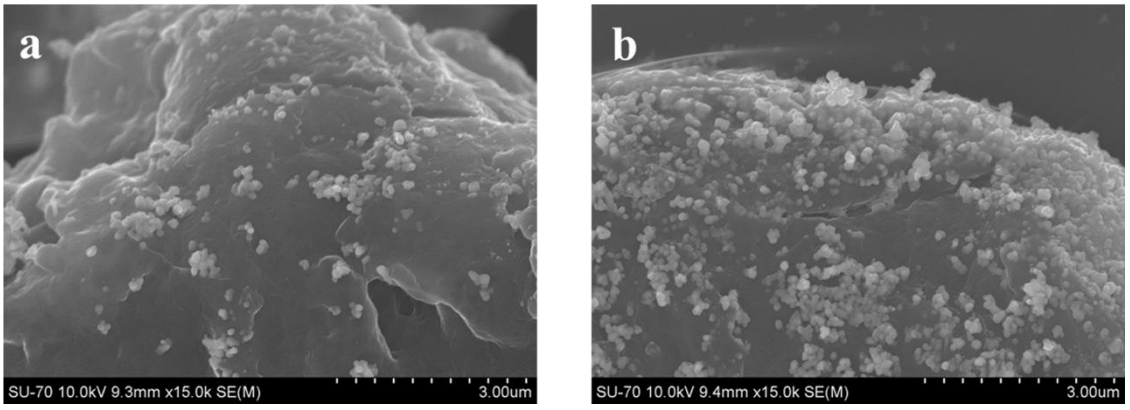

Fig. 1. SEM images of MCC-ZnO1 composite showing areas with low (a) and high (b) density of ZnO NPs.

In situ synthesis of ZnO NPs performed in the presence of biopolymers generated composites with higher content of Zn than those prepared by mixing the biopolymer with ZnO NPs (MCC-ZnO1). Using different biopolymers (MCC or CH) and variable reaction times (30 min or 2 h) three different composites were obtained with i*n situ* synthesis of ZnO NPs (MCC-ZnO2, MCC-ZnO3 and CH-ZnO4). SEM analysis of the nanocomposites showed that the nanoparticles tended to agglomerate at the surface of the polymer forming a compact ZnO NPs coating (Fig. 2). Unlike the commercial nanoparticles used in this work, which are nearly spherical-shape, the ZnO NPs obtained by *in situ* synthesis had a disc shape, with some of the NPs showing hexagonal facets. For the same time of reaction (30 min), *in situ* synthesis of ZnO NPs onto MCC or Chitosan (CH) occurred in a similar way. ZnO nanodiscs with similar diameter were obtained (129 ± 39 nm for MCC and 113 ± 33 nm for CH; values represent mean ± standard deviation) and the Zn content of the composites was not very different (13.5 for MCC and 12.9% for CH). Moreover, the ZnO NPs deposition efficiencies for MCC-ZnO2 and CH-ZnO4 were also similar, 85% and 81% respectively. This suggests that the type of matrix is not determinant in the *in situ* synthesis and growth of the ZnO NPs. By contrast, the reaction

time had relevant influence on the synthesis and deposition of ZnO NPs on the polymer. When the reaction time was increased from 30 min to 2 hours, larger ZnO particles were formed and the composite obtained showed higher Zn content (15.1 %) and higher deposition efficiency (94%). For the composites obtained by 30 min of reaction, the size of the nanoparticles was fairly uniform. For the composites prepared by 2 hour reaction, particles of variable diameters were formed (from 120 to 400 nm) and in some areas, the formation of a continuous ZnO film was observed (Fig. 2d). This means that long times of reaction favour a non-homogeneous growth of nanoparticles on the biopolymer. Although most of the nanoparticles were found on the surface of the polymer, it was possible to observe the presence of ZnO NPs also inside the cellulose fibers through the TEM analysis of the sample MCC-ZnO2 (Fig. S7, supporting information). This could be explained by considering that Zn precursor can penetrate onto the fibers and then undergo hydrolysis in the presence of NaOH solution producing ZnO NPs. Other authors also observed the formation of nanoparticles inside cellulose films or within regenerated cellulose fibers after in *situ* synthesis of ZnO NPs.[46,47] XRD pattern of the samples showed peaks correspondent to the polymers and to ZnO wurtzite phase confirming the presence of ZnO NPs on the composites (Fig. S8, supporting information). As expected, the UV-Vis spectra of MCC-ZnO2, MCC-ZnO3 and CH-ZnO4 presented the absorption edge associated to the energy gap of ZnO (Fig. S4, supporting information).

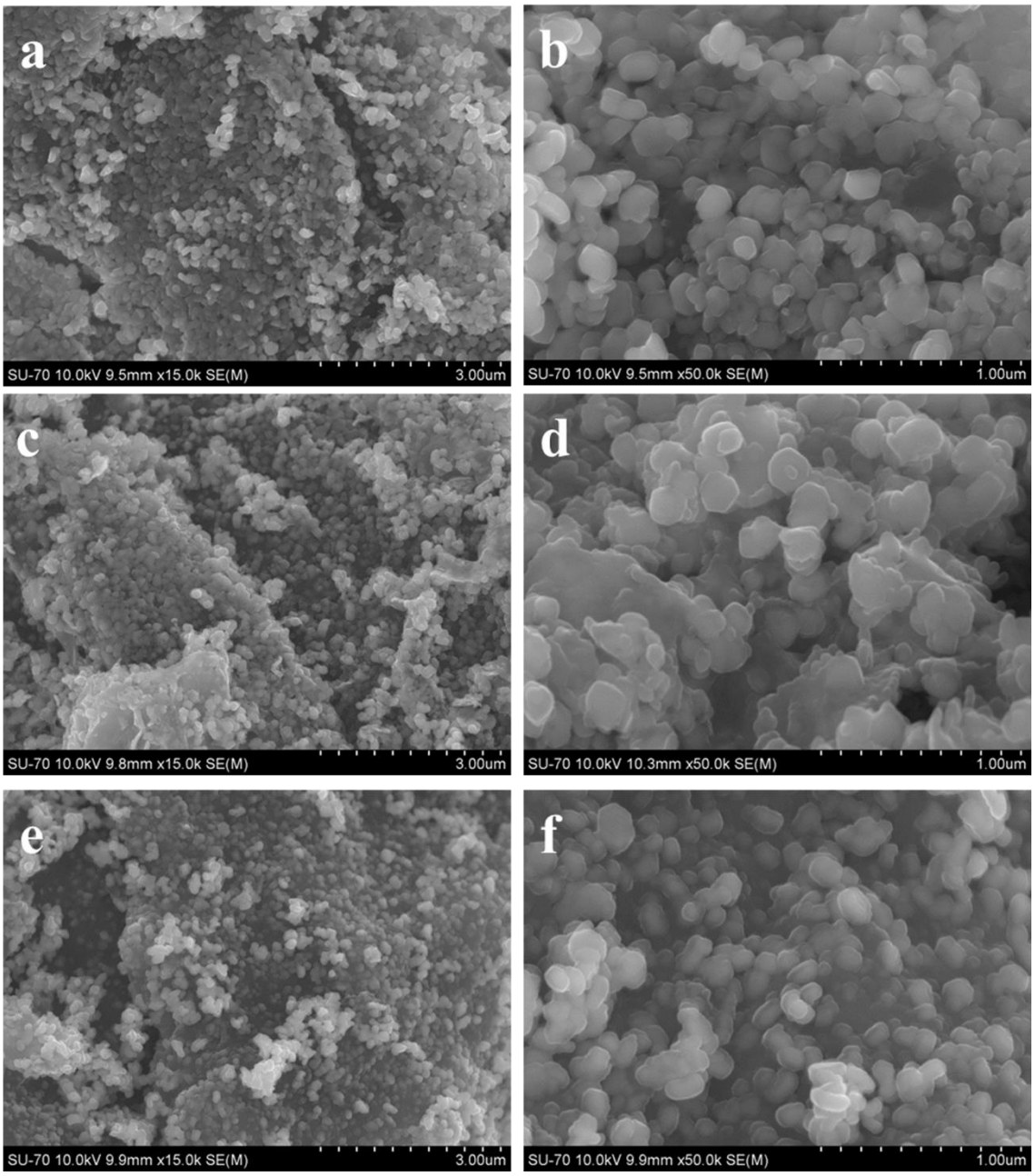

Fig. 2. SEM images of MCC-ZnO2 (a and b; 30 min reaction), MCC-ZnO3 (c and d; 2h reaction) and CH-ZnO4 (e and f; 30 min reaction) nanocomposites.

The composites MCC-ZnO2 and MCC-ZnO3 were further treated with a solution of alginate. Coating the composites with a layer of alginate (with opposite charge to the ZnO NPs) was tested to evaluate potentially slower Zn release. By SEM analysis of the composites obtained after treatment with alginate (MCC-ZnO2 ALG and MCC-ZnO3 ALG) it was not possible to identify a layer of polymer covering ZnO NPs (Fig. S9, supporting information). However, zeta potential measurements showed an increase of the surface charge of the

composites obtained after treatment with alginate as compared to the charge of the materials before treatment (Table 2). In the case of MCC-ZnO3 ALG a charge reversal was even observed. This suggested that the negatively charged alginate attached to the composites surface.

Table2

Zeta potential and pH of suspensions of MCC-ZnO composites treated and non-treated with alginate [a]

Sample	Zeta potential (mV)	pH
MCC-ZnO2	-18.6 ± 0.7	7.30 ± 0.10
MCC-ZnO2 ALG	-32.0 ± 3.2	7.78 ± 0.20
MCC-ZnO3	+ 6.0 ± 2.5	7.36 ± 0.20
MCC-ZnO3 ALG	-33.9 ± 2.1	7.75 ± 0.20

[a] Three replicate measurements were performed (values represent mean ± standard deviation). Both the zeta potential and the pH of composites treated with alginate were significantly different ($p < 0.05$) from the non-treated ones.

Entrapment of nutrients and active ingredients onto biopolymers is known to be helpful for controlled release of these compounds.[40,48] Having this in mind, a composite with high content of Zn (64.6%) was prepared by entrapment of ZnO NPs in a chitosan gel (G-CH-ZnO5). To prepare the composite a suspension of commercial ZnO NPs was added to a chitosan solution under agitation. According to Vasile et al.[40] chitosan amino groups interact with ZnO NPs and then the polymer chains wrap around the particles and as a result a chitosan gel is formed with ZnO NPs trapped inside. In fact, SEM analysis of the milled dried gel clearly showed areas where a film of chitosan was covering ZnO NPs (Fig. 3 a and b) Moreover, TEM images showed that the ZnO NPs were in fact wrapped by a polymer layer (Fig. 3 c and d). FTIR-ATR analyses also showed that there was a strong interaction between chitosan functional groups and ZnO surface (Fig. S10, supporting information). Chitosan displays characteristic vibrational bands at 3374 cm^{-1}(O-H stretching and N-H stretching in NH_2 group), 2868 cm^{-1} (CH_2, C-H

symmetric stretching), 1651 cm^{-1} (stretching vibration of C=O in amide), 1585 cm^{-1} (NH_2 bending), 1050-893 cm^{-1} (vibrations of C-O bonds). For composite G-CH-ZnO5 the band at 3374 cm^{-1} shifted to 3364 cm^{-1} and became more intense and broad. The peak at 1585 cm^{-1} correspondent to NH_2 bending also became more intense and shifted to lower wavelength (1553 cm^{-1}). The shift and the intensity increase of the FTIR peaks was attributed to the interaction of ZnO with OH and NH_2 groups of chitosan.[49] XRD of G-CH-ZnO5 showed the characteristic peaks of ZnO (*wurtzite*) as the main crystalline phase in the composite (Fig. S11, supporting information).

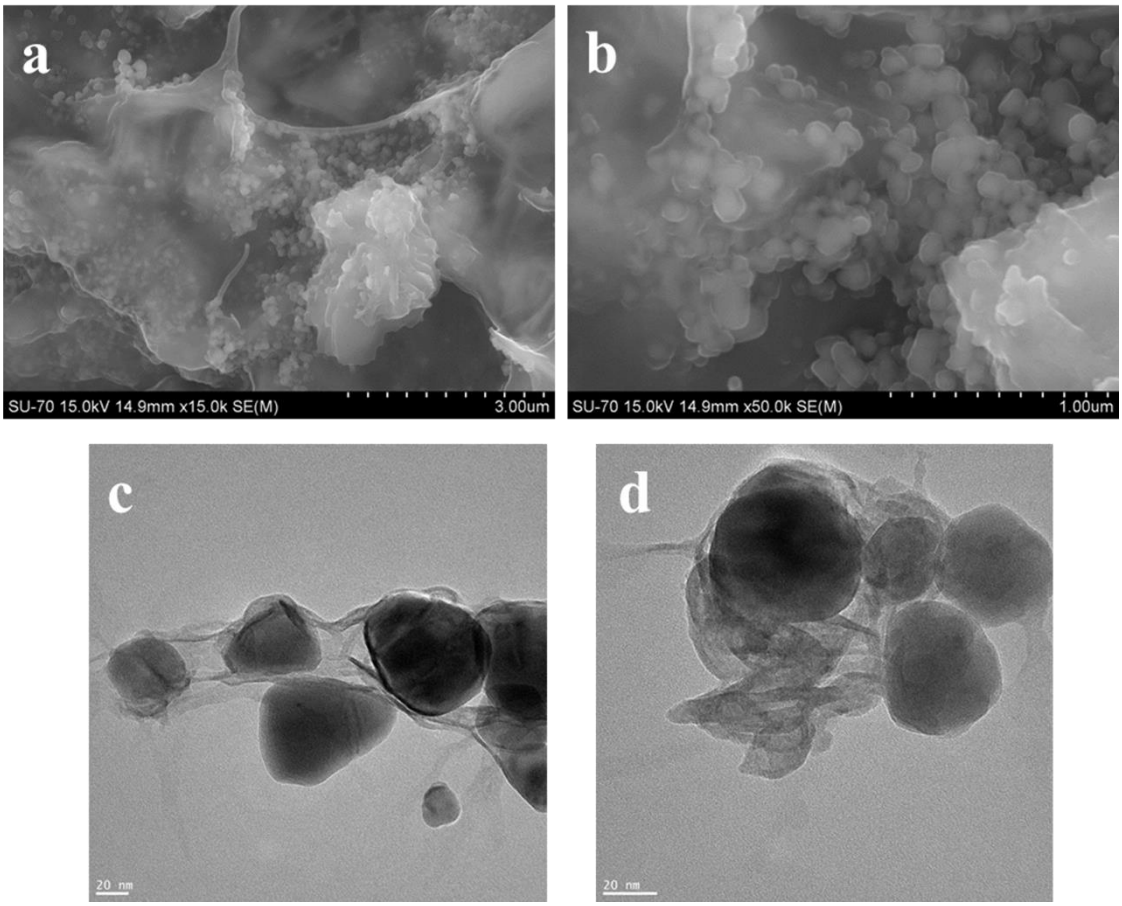

Fig. 3. SEM (a and b) and TEM (c and d) images of G-CH-ZnO5.

Other composites were prepared by entrapment of ZnO NPs inside a gel-like polymeric matrix. Two types of alginate beads containing ZnO NPs were prepared by dropping a suspension of ZnO NPs onto a solution of $CaCl_2$ (B-ALG6) or $ZnCl_2$ (B-ALG7). The wet beads exhibited spherical shape with a diameter of 1-3 mm (Fig. S12, supporting information). After air drying, the diameter of the beads decreased to about 1 mm; however, most of particles

maintained the spherical shape. XRD pattern for both alginate beads showed the characteristic peaks of ZnO *wurtzite* phase (Fig. S11, supporting information).

Zn content of B-ALG6 beads was found to be 11.8 % which means that 88% of the ZnO NPs that were in the suspension were entrapped by the polymer. SEM analysis of dried B-ALG6 beads showed a rough surface with some wrinkles and cracks (Fig. 4 a,c). In the high-resolution image of B-ALG6 it was possible to observe the ZnO NPs wrapped by alginate at the bead surface (Fig. 4e). Beads were cut in small pieces allowing the analysis of the interior of the beads. SEM images and Zn EDS mapping of this pieces showed that ZnO NPs were homogeneously distributed in the composite (Fig. S13, supporting information).

For B-ALG7 beads the Zn content (33.5 %) was more than two times higher than the obtained for B-ALG6 and the calculated efficiency of entrapment was higher than 100%. This was due to the fact that Zn present in the composite was not only derived from ZnO NPs but also from $ZnCl_2$ that acted to cross-link the alginate chains. SEM analyses of the surface of the beads showed not only the ZnO NPs but also abundant crystal structures (Fig. 4 d,f). It is possible that these crystals are $ZnCl_2$ that precipitated at the surface of the polymers or ZnO plates obtained by the growth of ZnO NPs in the presence of $ZnCl_2$. EDS mapping of Zn on a fragment of B-ALG7 bead revealed that this element is homogeneous distributed on the polymer surface (Fig. S14, supporting information).

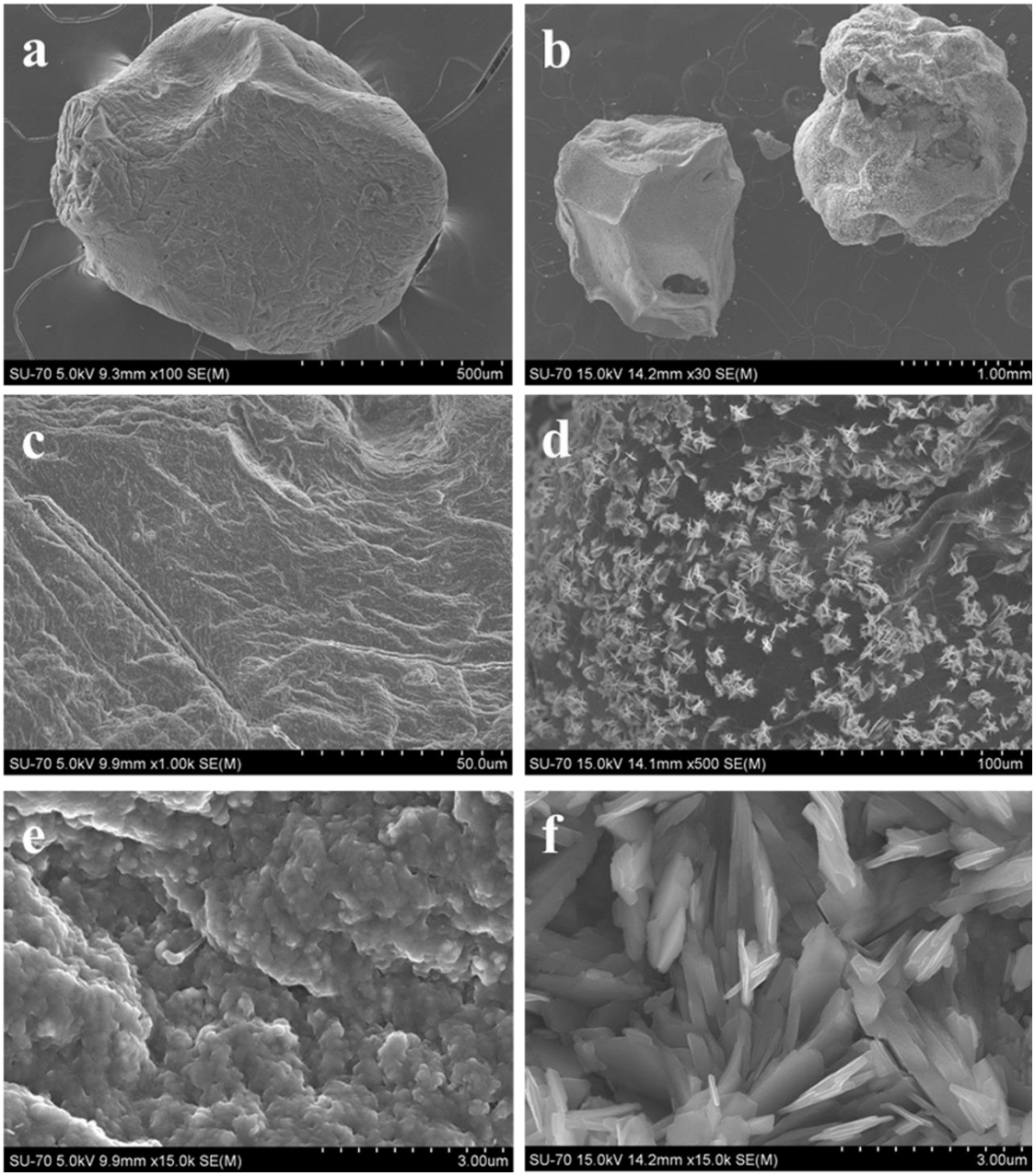

Fig. 4. SEM images of B-ALG6 (a, c and e) and B-ALG7 (b, d and f) nanocomposites.

The ZnO NPs deposition efficiencies for the composites G-CH-ZnO5 and B-ALG6 were 87 and 88% respectively. These values are similar to the deposition efficiencies of the composites obtained by *in situ* method (MCC-ZnO2, MCC-ZnO3 and CH-ZnO4) which were between 81 and 94%.

Finally, the pH of the suspensions of all the prepared composites was measured and values between 6.65 and 7.78 were obtained (Table S1, supporting information). The pH values of the suspensions of the MCC-ZnO composites treated with alginate (MCC-ZnO2 ALG and MCC-

ZnO3 ALG) were significantly higher ($p< 0.05$) than the pH of the suspensions of all remaining materials.

3.2 Extractability of Zn from all biopolymer composites in agricultural soils

The concentrations of 0.01 M $CaCl_2$ extractable Zn for soil LUFA 2.2 amended with ZnO composites, ZnO NPs and $ZnCl_2$ (100 mg of Zn per kg of dry soil) after 1 or 7 days of incubation was determined (Fig. 5). For all the materials including $ZnCl_2$, Zn extractability decreased with time. Lower Zn extractability over time in soils amended with $ZnCl_2$, $ZnSO_4$ or ZnO NPs was also reported by others researchers,[50,51] and is discussed further below. The extractable Zn for ZnO NPs amended soil was always lower than for $ZnCl_2$ amended soil suggesting that ZnO NPs were not completely dissolved after 7 days of incubation in soil. The Zn extractability in soil LUFA 2.2 amended with $ZnCl_2$ was significantly higher ($p<0.05$) than that of amendments with ZnO NPs composites.

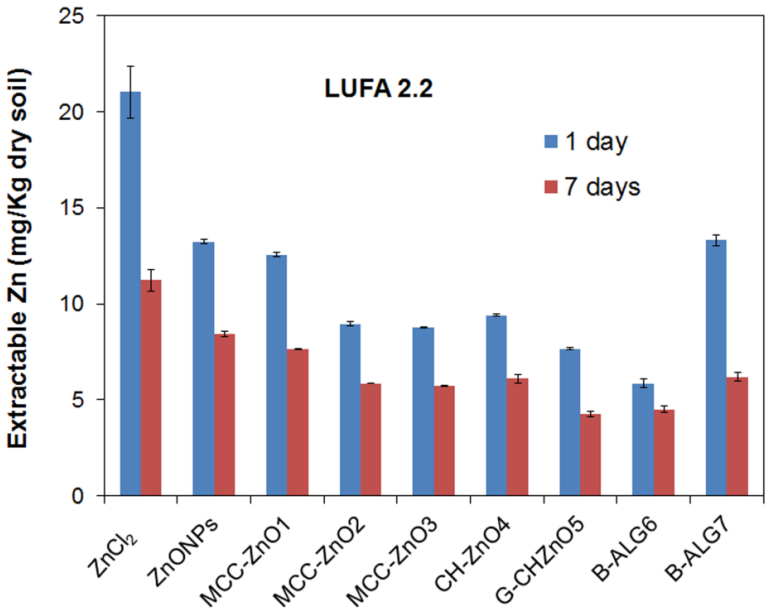

Fig. 5. Extractable Zn from soil LUFA 2.2 (pH = 6.3; 1.61% organic carbon) amended with $ZnCl_2$, ZnO NPs and ZnO composites, incubated for 1 or 7 days. Bars represent mean values and error bars represent standard deviation (n = 3).

With the exception of B-ALG7, all amendments with the ZnO NPs composites led to lower Zn extractability from soils than amendments with ZnO NPs alone (Fig. 5 and Table S2). In fact, Zn extractability decreased between (5.1 and 55.8%) suggesting a lower release of Zn on

soils when ZnO NPs were immobilized in a polymeric matrix. Although slightly lower, MCC-ZnO1 presented Zn release close to those observed for the ZnO NPs alone. This was attributed to the fact that the ZnO NPs on MCC-ZnO1 composite were mostly deposited onto the surface of MCC fibers and were only attached by electrostatic forces. When in the soil, the ZnO NPs could easily detach making the material behave similarly to that observed for non-immobilized ZnO NPs. Composites produced by *in situ* synthesis (MCC-ZnO2, MCC-ZnO3 and CH-ZnO4) presented a lower Zn release (extractability was 1.2-1.4 lower) compared with MCC-ZnO1. In this case, is possible that most of the ZnO NPs were attached to the polymer by chemical bonds or trapped between polymeric fibbers making more difficult the Zn release. However, the release of Zn was similar for MCC-ZnO2, MCC-ZnO3 and CH-ZnO4 showing that the type of polymeric substrate and size of the ZnO NPs had no decisive role on the Zn release for the materials prepared by *in situ* method.

MCC-ZnO2 ALG and MCC-ZnO3 ALG (prepared by the treatment of MCC-ZnO composites with alginate) showed Zn release levels similar to the untreated composites (Table S2); however, it is possible to see a trend of lower release (2-10% less) for the treated materials.

The materials showing the slowest Zn release were those prepared by entrapment of ZnO NPs in a gel structure (G-CHZnO5 and B-ALG6). Clearly, the extractability of Zn from soil LUFA 2.2 amended with B-ALG6 alginate beads was two and three times lower than the extractability of the soil amended with ZnO NPs and $ZnCl_2$ respectively. Although the Zn extractability for G-CHZnO5 in the end of day 1 was higher than for B-ALG6 it became similar after 7 days of incubation. For these materials, water molecules need to diffuse through pores and channels of the polymeric gel to get in contact with ZnO NPs and to dissolve them. After that, the ionic Zn must diffuse throughout of the gel to be released onto soil pore water. This process hinders a rapid dissolution of ZnO NPs.

It should be mentioned that B-ALG7 alginate beads that were produced using $ZnCl_2$ as crosslinking agent instead of $CaCl_2$ presented almost the same Zn release after 1 day of incubation as the amendment with ZnO NPs alone. This could be explained by the fact that at least half of the Zn present in the composite was not in ZnO NPs form. In fact, part of the zinc was founded at alginate chains (as crosslinking agent) or adsorbed at the surface of the polymer.

It was clear that the fraction of extractable Zn was significantly higher in soil LUFA 2.1 (44-88 % of added Zn content) then in soil LUFA 2.2 (5-21 %) for all the materials, including $ZnCl_2$ (Fig. 6 and Table S3). This was attributed to the lower pH (5.2) and lower organic matter content (0.71% organic carbon) of soil LUFA 2.1 compared with LUFA 2.2 (pH = 6.3; 1.61% organic carbon). Other authors also reported that soils with low pH and low organic matter

content show a higher lability of Zn.[52,53] The Zn extractability in soil LUFA 2.1 amended with $ZnCl_2$ was significantly higher ($p<0.05$) than that of ZnO NPs composites and of ZnO NPs alone.

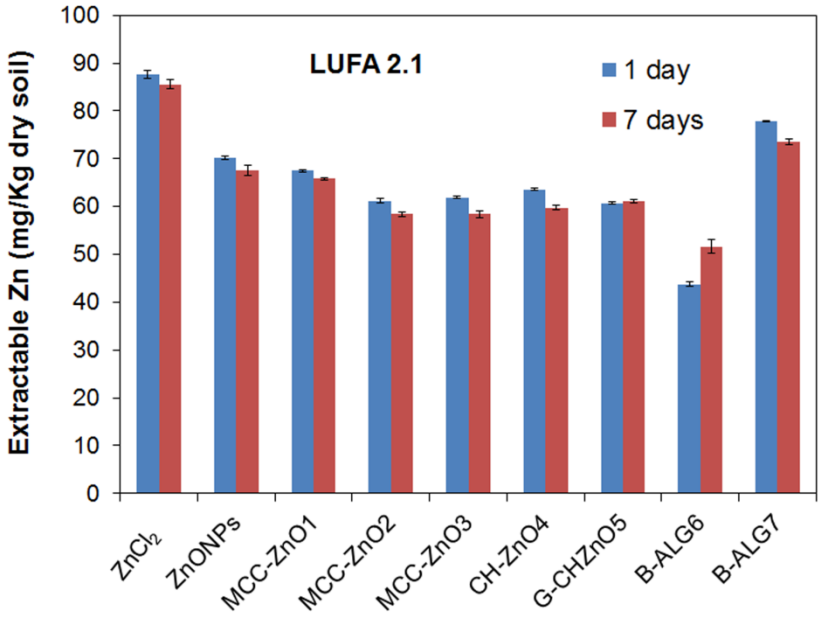

Fig. 6. Extractable Zn from soil LUFA 2.1 (pH = 5.2; 0.71% organic carbon) amended with $ZnCl_2$, ZnO NPs and ZnO composites, incubated for 1 or 7 days. Bars represent mean values and error bars represent standard deviation (n = 3).

For both LUFA 2.2 and LUFA 2.1 soils all the composites presented lower Zn extractability compared with ZnO NPs, with the exception of B-ALG7. However, the differences in Zn release between the different composites were clearly smaller for soil LUFA 2.1. This shows that the percentage and rate of Zn release from the composites is not only determined by the type of attachment of the ZnO NPs to the polymer but also by soil properties, particularly pH and organic carbon content. It was clear that the alginate beads containing ZnO NPs prepared by crosslinking with $CaCl_2$ (B-ALG6) were the materials that presented the lower Zn release in both soils.

3.3 Extractability of Zn from agricultural soils dosed with ZnONPs/alginate beads composites along 30 days

A soil test with a longer incubation time (30 days) and more data points (day 1, 4, 7, 15 and 30) was performed to further evaluate the Zn release behaviour from B-ALG6 along time. The behaviour of B-ALG6 was compared with that observed for $ZnCl_2$ in the same period of time.

The concentration of $CaCl_2$ extractable Zn from soils DE (pH = 6.9) and VV (pH = 7) amended with $ZnCl_2$ was between 0.736 mg/kg (day 1) and 0.09 mg/kg (day 30). For B-ALG6 the concentration of extractable Zn was below the detection limit of ICP-MS analysis from day 1 to day 30 (Table S4, supporting information). This suggests that these materials may not be efficient for controlled release of Zn in neutral/alkaline soils.

The concentrations of 0.01 M $CaCl_2$ extractable Zn for soil LUFA 2.2 amended with B-ALG6 and $ZnCl_2$ over 30 days are shown in Fig. 7 (a). The materials exhibited distinct behaviour in relation to extractable Zn. In the $ZnCl_2$ amended soil, the extractable Zn was high in the first day and then showed a fast decrease with time. A decrease of 60% in the extractable Zn was observed from day 1 to day 15 of incubation in soil. After 15 days of incubation the extractable Zn further decreased but at a slower rate. This behaviour could be a result of an initial rehydration of the soil, followed by ionic Zn micropore diffusion, and further complexation in soil by organic matter (SOM) or incorporation/precipitation of Zn in/onto stable oxide mineral phases.[24,25]

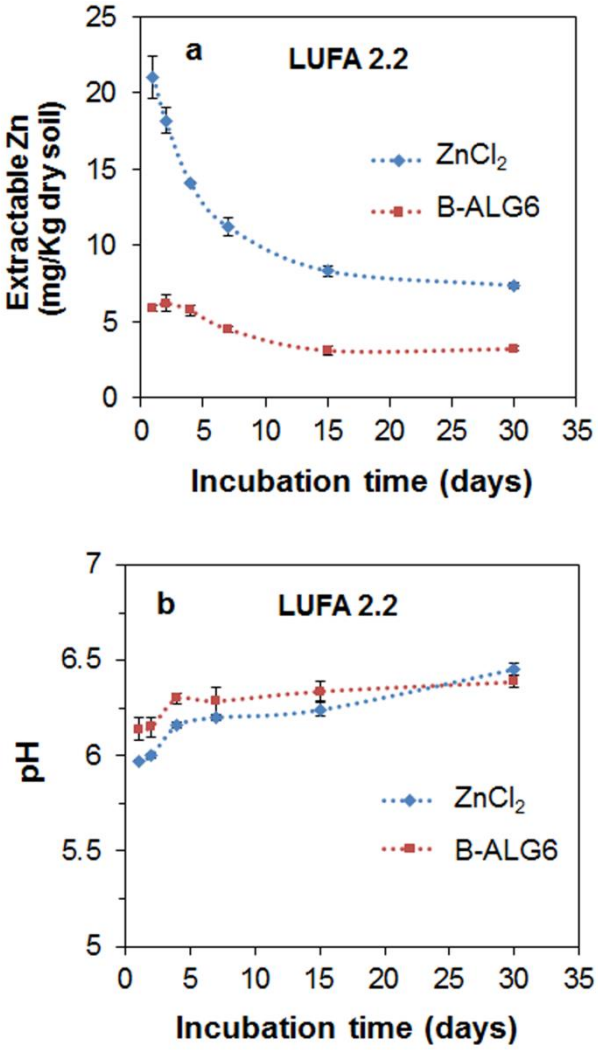

Fig. 7. (a) Extractable Zn from soil LUFA 2.2. amended with $ZnCl_2$ and B-ALG6 as function of time (b) pH of the extracts. To better visualize the trend of the results the points in the graphics were joined with dotted lines. Error bars represent standard deviation of the mean (n = 3).

In the case of B-ALG6 amended soil there is a small increase of Zn extractability from day 1 to day 2. This was followed by a period of slow decrease of Zn extractability until a plateau is reached in the end of 15 days. The increase in Zn extractability in the first two days suggested that the ZnO NPs were becoming more extractable as a result of acid-promoted dissolution of ZnO NPs (eq. (1)).

$$ZnO\ (s) + 2H^{+}\ (aq) \leftrightarrow Zn^{2+}\ (aq) + H_2O\ (l) \qquad (1)$$

At the end of 30 days of incubation after soil dosing, the extractable Zn for B-ALG6 amended soil was still lower than for $ZnCl_2$ amended soil suggesting that ZnO NPs dissolution was not complete in this period of time. It was also possible to observe that the pH of the extracts

of B-ALG6 amended soil in the first 15 days was higher than for soil amended with $ZnCl_2$ (Fig. 7b). This can be also attributed to the acidic dissolution of ZnO NPs, as described by eq.(1).

Similar trends were observed for LUFA 2.1 amended soils (Fig. 8 a). In the soil amended with $ZnCl_2$, 88% of the Zn added to the soil was extractable in the first day, while in the soil amended with B-ALG6 only 44% was extractable. The $ZnCl_2$ amended soils showed a decrease in the extractable Zn over 15 days, whereas the B-ALG6 amended soils presented a small increase in the extractable Zn in the first 7 days and after that the concentration of extractable Zn was almost constant. For soil LUFA 2.1 amended with B-ALG6 the period of time where an increase of Zn extractability is registered is higher (7 days, against 2 days in soil LUFA 2.2). This was attributed to the more acidic nature of this soil (pH of 5.2) that can promote faster dissolution of ZnO NPs (eq. (1)).

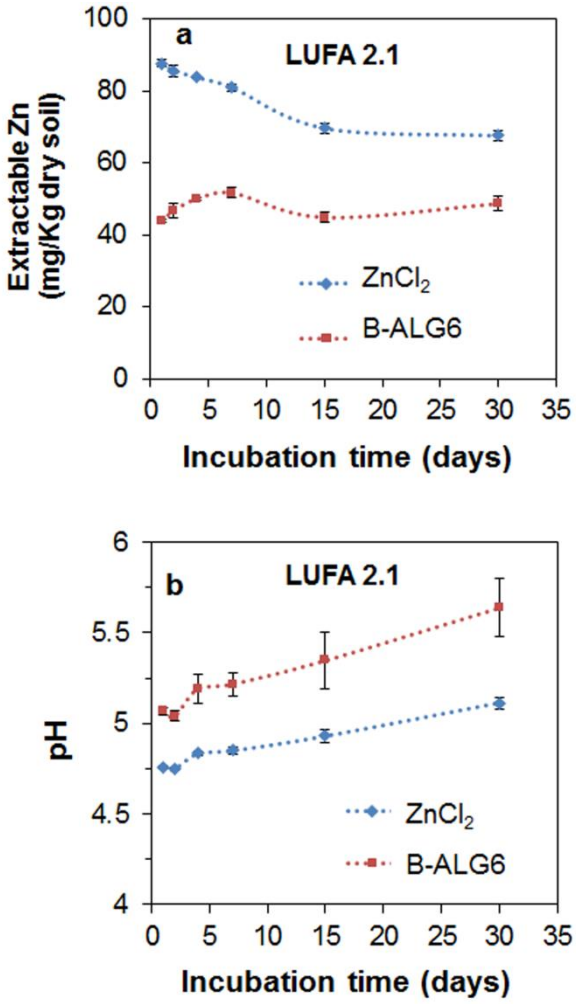

Fig. 8. (a) Extractable Zn from soil LUFA 2.1. amended with $ZnCl_2$ and B-ALG6 as function of time (b) pH of the extracts. To better visualize the trend of the results the points in the graphics were joined with dotted lines. Error bars represent standard deviation of the mean (n = 3).

As clearly shown in Figures 7 and 8, difference between the pH values of the extracts of B-ALG6 amended soil and the extracts of $ZnCl_2$ amended soil was higher in soil LUFA 2.1 than in soil LUFA 2.2. This could be related with the degradation of the polymeric matrix in this soil with the formation of products with alkaline character. Kanakaraju et al.[54] also reported an increase of the pH of a solution containing alginate beads with time and the degradation of alginate was pointed out as one of the possible causes for the pH rise.

3.4 Controlled release of Zn from ZnO NPs/alginate beads for Maize fertilization in acidic soil

To investigate the potential of ZnO NPs alginate beads (B-ALG6) to be use in Zn-deficient acidic soil as a Zn source for maize, the growth of maize was assessed in LUFA 2.1 supplied with different Zn sources ($ZnCl_2$, ZnO NPs or B-ALG6), at 30 or 100 mg of Zn per kg of dry soil. Controls (soil amended with ultrapure water, or with the equivalent mass of alginate as what was amended in the B-ALG6 treatment) were also run in parallel.

As described for the extractable Zn in soils incubated without plants, adding Zn to LUFA 2.1 increased the Zn concentration in the pore water for all days in comparison to the non-zinc controls (see Fig. 9 a and Table S5). While this increase was high at day 2, it stabilized at day 29 as it was 2-4 times higher for all the 30 mg/Kg amendments, and 9-17 time higher for the 100 mg/Kg amendments (Table S5). The zinc concentrations in the pore water decreased from day 2 to day 29 for all conditions. While this decrease was the highest for $ZnCl_2$ treatments (94% and 91% of decrease for the 30 ppm and 100 ppm amendment, respectively), the B-ALG6 treatment was the one that showed the lowest decrease (72 and 79% of decrease for the 30 ppm and 100 ppm treatment, respectively), indicating that the loss of Zn by leaching in soil for that treatment was lowered (see Table S5). This decrease in Zn pore water concentrations over time seems to be driven by its pH increase (Figure 9a) as these traits significantly correlates together (Figure S15a).

The $CaCl_2$ extractable Zn concentrations in the bulk soil (far away from the main root systems) follow similar trends, with higher Zn amendment increasing the extractable Zn, following the trend $ZnCl_2$ = ZnO NPs > B-ALG6 (Figure 9b).

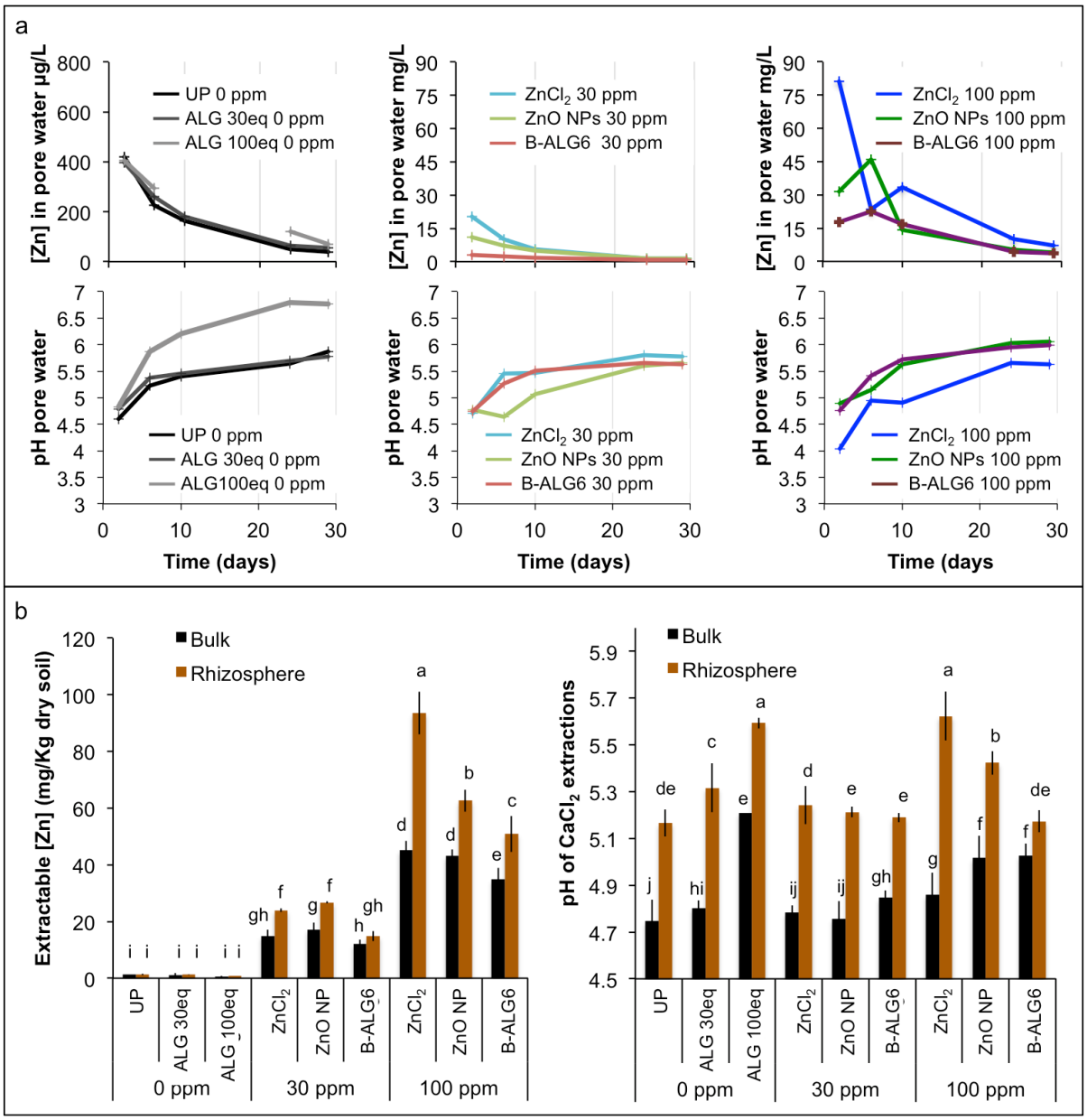

Fig. 9. (a) Zinc concentration in LUFA 2.1 pore water along with its pH over the time of maize growth for 29 days, and (b) extractable Zn at day 29 in both the bulk or rhizosphere soil along with its pH. UP is the control. ALG 30eq and ALG 100eq are the LUFA 2.1 soil dosed with equivalent ALG doses as the composite treatments. Zn was amended as $ZnCl_2$, ZnO NPs, B-ALG6 at 30 or 100 mg of zinc per Kg of dry soil. Different letters indicate of different means (ANOVA, $p<0.05$)

These differences among treatments are even clearer in the rhizosphere soil, where all the overall extractable Zn concentrations are higher than in the bulk soils. This highlights the great influence of the roots exudation on the Zn bioavailability in the rhizosphere. It is noteworthy that in the rhizosphere, all of the pH (1:10 soil:0.01 M $CaCl_2$) were also significantly higher than in the bulk soils (Figure 9 b), which was surprising giving the higher extractable Zn concentrations. Indeed, while extractable Zn concentrations were negatively correlated with the pH in the bulk soil, this correlation was positive in the rhizosphere soil (Figure S15b). This indicates that plants and their microbiome can release compounds that increase Zn bioavailability in a non-pH dependant manner in the rhizosphere, as exo-polysaccharides, organic matter, organic acids and/or chelators.[55] Similar conclusions have been made while studying Cu bioavailability in the rhizosphere.[56] This underlies the need of considering the fate of (micro)nutrients in the rhizosphere (fate at the root-soil interface), while studying soil physical-chemical parameters influencing (micro)nutrients bioavailability. Reactions in the rhizosphere, will likely be different than in the bulk soil, changing the predictions[57] of micronutrient bioavailability and biogeochemical cycling in the latter when plants are present.

The highest pH (>5.5) observed for $ZnCl_2$ and ZnO NPs 100 ppm could be a response of the plant to a (too) high bioavailable zinc concentration in its roots vicinity,[55] that induce toxic impacts on the plant growth. Indeed, the dry biomass of the maize plant grown on these soils seems to validate this hypothesis. Maize growing on the soils presenting the highest extractable Zn ($ZnCl_2$ and ZnO NPs dosed at 100mg/Kg) produced less biomass than the control without Zn addition (Figure 10). The smaller plants and biomass observed for the alginate control could be due to an increase of pH induced by the alginate presence that may reduce bioavailability of other micronutrients. These results illustrate well how too low of a micronutrient bioavailability impair plant growth, while too much of it induce toxic impacts.

Of all the treatments, B-ALG6 100 ppm was the only one showing an increase in plant biomass and density, slightly improving the plant growth. It is noteworthy that the fact that this increase was not statistically significant was likely because the experiment was stopped at 29 days, while Zn deficiency effects on the biomass appears in latter stages of the plant growth. This could explain why significant differences in biomass where not observed in the B-ALG6 treated soil in comparison with the control soil, while the conditions for Zn deficiencies in LUFA 2.1 were met (Zn pore water <0. 5 mg/L[14] and <1 ppm of DTPA-extractable Zn).[23] However, some early signs of Zn deficiency (chlorisis and yellow margins) were observed on the maize leaves growing on LUFA 2.1 soil (see Figure S16), that did not appear when grown on the zinc-amended soils. Signs of toxicity were observed for the ZnO NPs and $ZnCl_2$

treatments at 100 mg/Kg of concentration (see Figure S16). From all the treatments, B-ALG6 dosed at 100 mg of Zn per Kg of soil was the only treatment that slightly improved plant growth, while not presenting any signs of Zn deficiencies nor metallic toxicity.

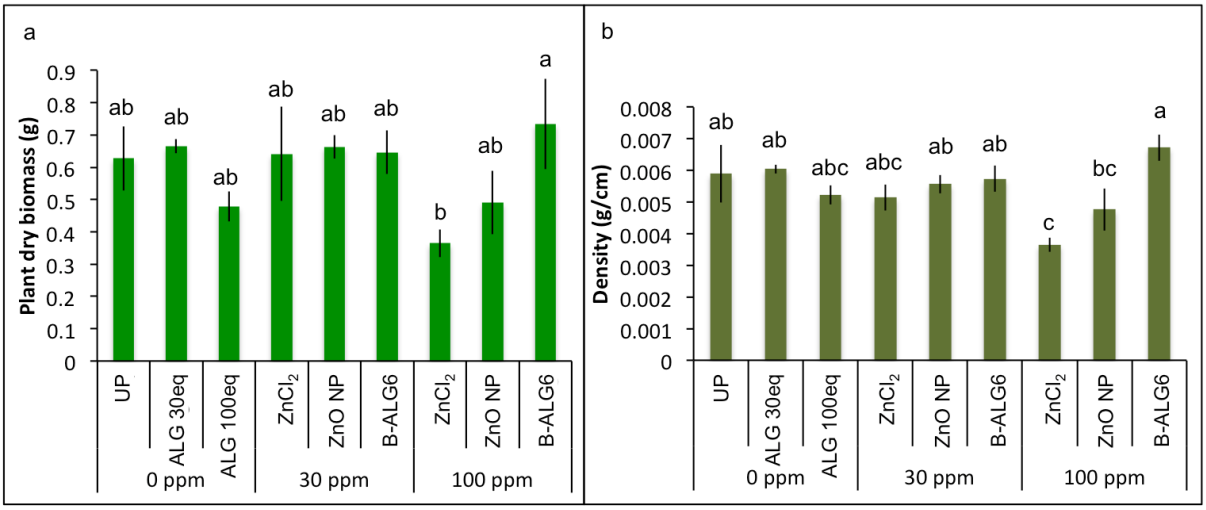

Fig. 10. Maize after 29 days of growth in LUFA 2.1 amended with different treatments and (a) their biomass or (b) their density (shoot biomass normalized by the leaves length). Different letters indicate of different means (ANOVA, $p<0.05$)

4. CONCLUSIONS

These results illustrate how precise the strategies for fertilisation have to be to meet plants (micro)nutrients needs, while avoiding waste generation, water contamination, metal leaching in the environment, and toxic effects on soil organisms. This study demonstrates that the immobilization of ZnO NPs onto natural polymers is a way to produce materials that release Zn in soils in a controlled manner. The composites of biopolymers and ZnO NPs produced here showed lower Zn release in acidic soil than $ZnCl_2$ or ZnO NPs alone, with Zn release which was soils- and polymer- type dependent. Our results suggest that ZnO NPs immobilized onto alginate beads (prepared by crosslinking with $CaCl_2$) can be used for controlled release of Zn in agricultural soils. This ZnO NPs/alginate beads could thus meet the Zn needs of maize plant on the acidic soil LUFA 2.1. In comparison, conventional salts of $ZnCl_2$ have to be added in the soil in high quantities to meet the plant needs after its leaching in the soil, which can induce toxic responses at the earlier stage of the plant growth, and represent a large waste of materials.

This study demonstrates that fertilisers that can slowly release micronutrient in a controlled manner, as the one presented here, can supply enough Zn for a plant to grow well, while reducing the Zn losses. Because of this long-term release, this kind of material could be applied once in the soil and be reused for several crop cycling.

Further studies of Zn release from these types of materials should be performed for longer times to better understand the fate of these materials in the bulk soil in comparison to the soil of the rhizosphere, to ensure the safety of materials for use in agri-food production. Scalability and cost are also important parameters that must be considered when analysing the viability of such new fertilizers from a commercial point of view.

ASSOCIATED CONTENT

Supporting Information

SEM and TEM images and particle size distribution histogram for commercial ZnO NPs ; XRD pattern for ZnO NPs and for ZnO composites; UV-visible spectra of ZnO NPs and ZnO composites; EDS spectrum of MCC-ZnO1; TEM image of MCC-ZnO2; SEM images of MCC-ZnO2 ALG and MCC-ZnO3 ALG; FTIR-ATR spectra of G-CH-ZnO5; Photographs of alginate beads and SEM images of the interior of the beads; pH values of suspensions of all the materials; Extractable Zn from soils DE and VV amended with B-ALG6 or $ZnCl_2$ (30 days incubation test); Photographs showing Zn deficiencies in maize grow; Correlations between Zn concentration in pore water or bulk soil or rhizosphere soil and pH; Decrease of Zn concentration in soil pore water between day 2 and day 29 for the different treatments.

ACKNOWLEDGMENTS

Thanks are due for the financial support to CESAM (UID/AMB/50017 - POCI-01-0145-FEDER-007638), to Portuguese FCT/MCTES through national funds (PIDDAC), and the co-funding by the FEDER, within the PT2020 Partnership Agreement and Compete 2020, under project NanoFertil (references: POCI-01-0145-FEDER-016749 and PTDC/AGR-PRO/6262/2014). S. M. Rodrigues also acknowledges the financial support from FCT (Project IF/01637/2013). Tito Trindade and Natércia Martins thank the CICECO-Aveiro Institute of Materials (Ref. FCT UID /CTM /50011/2019), financed by national funds through the FCT/MEC and when appropriate co-financed by FEDER under the PT2020 Partnership Agreement. Natércia Martins is funded by National funds (OE), through FCT- Fundação para a Ciência e Tecnologia, I.P., in the scope of the framework contract foreseen in the numbers 4,

5 and 6 of the article 23, of the Decree-Law 57/2016, of August 29, changed by the law 57/2017, of July 19.

REFERENCES

(1) Feiner, L. F. Nanoelectronics: Crossing Boundaries and Borders. *Nat. Nanotechnol.* **2006**, *1* , 91–92.

(2) Bera, R.; Dutta, A.; Kundu, S.; Polshettiwar, V.; Patra, A. Design of a CdS/CdSe Heterostructure for Efficient H2 Generation and Photovoltaic Applications. *J. Phys. Chem. C* **2018**, *122*, 12158–12167.

(3) Fonseca-Santos, B.; Gremião, M. P. D.; Chorilli, M. Nanotechnology-Based Drug Delivery Systems for the Treatment of Alzheimer's Disease. *Int. J. Nanomedicine.* **2015**, *10*, 4981–5003.

(4) Jiang, B.; Lian, L.; Xing, Y.; Zhang, N.; Chen, Y.; Lu, P.; Zhang, D. Advances of Magnetic Nanoparticles in Environmental Application: Environmental Remediation and (Bio)Sensors as Case Studies. *Environ. Sci. Pollut. Res.* **2018**, *25*, 30863–30879.

(5) Rodrigues, S. M.; Demokritou, P.; Dokoozlian, N.; Hendren, C. O.; Karn, B.; Mauter, M. S.; Sadik, O. A.; Safarpour, M.; Unrine, J. M.; Viers, J.; et al. Nanotechnology for Sustainable Food Production: Promising Opportunities and Scientific Challenges. *Environ. Sci.: Nano*. **2017**, *4*, 767–781.

(6) Khot, L. R.; Sankaran, S.; Maja, J. M.; Ehsani, R.; Schuster, E. W. Applications of Nanomaterials in Agricultural Production and Crop Protection: A Review. *Crop Prot.* **2012**, *35*, 64–70.

(7) Baker, S.; Volova, T.; Prudnikova, S. V.; Satish, S.; Prasad M.N., N. Nanoagroparticles Emerging Trends and Future Prospect in Modern Agriculture System. *Environ. Toxicol. Pharmacol.* **2017**, *53*, 10–17.

(8) Kah, M.; Kookana, R. S.; Gogos, A.; Bucheli, T. D. A Critical Evaluation of Nanopesticides and Nanofertilizers Against Their Conventional Analogues. *Nat. Nanotechnol.* **2018**, *13*, 677–684.

(9) Kumaraswamy, R. V.; Kumari, S.; Choudhary, R. C.; Pal, A.; Raliya, R.; Biswas, P.; Saharan, V. Engineered Chitosan Based Nanomaterials: Bioactivities, Mechanisms and Perspectives in Plant Protection and Growth. *Int. J. Biol. Macromol.* **2018**, *113*, 494–506.

(10) Raliya, R.; Saharan, V.; Dimkpa, C.; Biswas, P. Nanofertilizer for Precision and Sustainable Agriculture: Current State and Future Perspectives. *J. Agric. Food Chem.* **2018**, *66*, 6487–6503.

(11) Servin, A. D.; White, J. C. Nanotechnology in Agriculture: Next Steps for Understanding Engineered Nanoparticle Exposure and Risk. *NanoImpact* **2016**, *1*, 9–12.

(12) Savassa, S. M.; Duran, N. M.; Rodrigues, E. S.; de Almeida, E.; van Gestel, C. A. M.; Bompadre, T. F. V.; P. de Carvalho, H. W. Effects of ZnO Nanoparticles on Phaseolus Vulgaris Germination and Seedling Development Determined by X-Ray Spectroscopy . *ACS Appl. Nano Mater.* **2018**, *1*, 6414–6426.

(13) Dimkpa, C. O.; Bindraban, P. S. Nanofertilizers: New Products for the Industry? *J. Agric. Food Chem.* **2018**, *66*, 6462–6473.

(14) Liu, R.; Lal, R. Potentials of Engineered Nanoparticles as Fertilizers for Increasing Agronomic Productions. *Sci. Total Environ.* **2015**, *514*, 131–139.

(15) Chhipa, H. Nanofertilizers and Nanopesticides for Agriculture. *Environ. Chem. Lett.* **2017**, *15*, 15–22.

(16) Achari, G. A.; Kowshik, M. Recent Developments on Nanotechnology in Agriculture:

Plant Mineral Nutrition, Health, and Interactions with Soil Microflora. *J. Agric. Food Chem.* **2018**, *33*, 8647–8661.

(17) Cicek, S.; Nadaroglu, H. The Use of Nanotechnology in the Agriculture. *Adv. Nano Res.* **2015**, *3*, 207–223.

(18) Kabiri, S.; Degryse, F.; Tran, D. N. H.; Da Silva, R. C.; McLaughlin, M. J.; Losic, D. Graphene Oxide: A New Carrier for Slow Release of Plant Micronutrients. *ACS Appl. Mater. Interfaces* **2017**, *9*, 43325–43335.

(19) Azeem, B.; Kushaari, K.; Man, Z. B.; Basit, A.; Thanh, T. H. Review on Materials & Methods to Produce Controlled Release Coated Urea Fertilizer. *J. of Controlled Release.* **2014**, *181*, 11–21.

(20) Reddy Pullagurala, V. L.; Adisa, I. O.; Rawat, S.; Kim, B.; Barrios, A. C.; Medina-Velo, I. A.; Hernandez-Viezcas, J. A.; Peralta-Videa, J. R.; Gardea-Torresdey, J. L. Finding the Conditions for the Beneficial Use of ZnO Nanoparticles towards Plants-A Review. *Environmental Pollution*. **2018**, *241*, 1175–1181.

(21) Cakmak, I.; Kutman, U. B. Agronomic Biofortification of Cereals with Zinc: A Review. *Eur. J. Soil Sci.* **2018**, *69*, 172–180.

(22) Hotz, C. The Potential to Improve Zinc Status through Biofortification of Staple Food Crops with Zinc. *Food Nutr. Bull.* **2009**, *30*, 172-178.

(23) Lindsay, W. L.; Norvell, W. A. Development of a DTPA Soil Test for Zinc, Iron, Manganese, and Copper. *Soil Sci. Soc. Am. J.* **1978**, *42*, 421.

(24) Voegelin, A.; Scheinost, A. C.; Bühlmann, K.; Barmettler, K.; Kretzschmar, R. Slow Formation and Dissolution of Zn Precipitates in Soil: A Combined Column-Transport and XAFS Study. *Environ. Sci. Technol.* **2002**, *36*, 3749–3754.

(25) Opfergelt, S.; Cornélis, J. T.; Houben, D.; Givron, C.; Burton, K. W.; Mattielli, N. The Influence of Weathering and Soil Organic Matter on Zn Isotopes in Soils. *Chem. Geol.* **2017**, *466*, 140–148.

(26) Cakmak, I. Enrichment of Cereal Grains with Zinc: Agronomic or Genetic Biofortification? *Plant and Soil*. **2008**, *302*, 1–17.

(27) Alloway, B. J. Soil Factors Associated with Zinc Deficiency in Crops and Humans. *Environ. Geochem.Health* **2009**, *31*, 537–548.

(28) Zhao, A. Q.; Tian, X. H.; Chen, Y. L.; Li, S. Application of ZnSO4 or Zn-EDTA Fertilizer to a Calcareous Soil: Zn Diffusion in Soil and Its Uptake by Wheat Plants. *J. Sci. Food Agric.* **2016**, *96*, 1484–1491.

(29) Lin, D.; Xing, B. Phytotoxicity of Nanoparticles: Inhibition of Seed Germination and Root Growth. *Environ. Pollut.* **2007**, *150*, 243–250.

(30) Yang, Z.; Chen, J.; Dou, R.; Gao, X.; Mao, C.; Wang, L. Assessment of the Phytotoxicity of Metal Oxide Nanoparticles on Two Crop Plants, Maize (Zea Mays L.) and Rice (Oryza Sativa L.). *Int. J. Environ. Res. Public Health* **2015**, *12*, 15100–15109.

(31) Elmer, W. H.; White, J. C. The Use of Metallic Oxide Nanoparticles to Enhance Growth of Tomatoes and Eggplants in Disease Infested Soil or Soilless Medium. *Environ. Sci.: Nano* **2016**, *3*, 1072–1079.

(32) Wang, P.; Menzies, N. W.; Lombi, E.; McKenna, B. A.; Johannessen, B.; Glover, C. J.; Kappen, P.; Kopittke, P. M. Fate of ZnO Nanoparticles in Soils and Cowpea (Vigna Unguiculata). *Environ. Sci. Technol.* **2013**, *47*, 13822–13830.

(33) Juárez-Maldonado, A.; Ortega-Ortíz, H.; Pérez-Labrada, F.; Cadenas-Pliego, G.; Benavides-Mendoza, A. Cu Nanoparticles Absorbed on Chitosan Hydrogels Positively Alter Morphological, Production, and Quality Characteristics of Tomato. *J. Appl. Bot. Food Qual.* **2016**, *89*, 183–189.

(34) Sharif, R.; Mujtaba, M.; Rahman, M. U.; Shalmani, A.; Ahmad, H.; Anwar, T.; Tianchan, D.; Wang, X. The Multifunctional Role of Chitosan in Horticultural Crops; a Review. *Molecules*. **2018**, *23*, 872.

(35) Perez, J. J.; Francois, N. J. Chitosan-Starch Beads Prepared by Ionotropic Gelation as Potential Matrices for Controlled Release of Fertilizers. *Carbohydr. Polym.* **2016**, *148*, 134–142.
(36) Jamnongkan, T.; Kaewpirom, S. Potassium Release Kinetics and Water Retention of Controlled-Release Fertilizers Based on Chitosan Hydrogels. *J. Polym. Environ.* **2010**, *18*, 413–421.
(37) Ul-Islam, M.; Khattak, W. A.; Ullah, M. W.; Khan, S.; Park, J. K. Synthesis of Regenerated Bacterial Cellulose-Zinc Oxide Nanocomposite Films for Biomedical Applications. *Cellulose* **2014**, *21*, 433–447.
(38) Gao, X.; Spielman-Sun, E.; Rodrigues, S. M.; Casman, E. A.; Lowry, G. V. Time and Nanoparticle Concentration Affect the Extractability of Cu from CuO NP-Amended Soil. *Environ. Sci. Technol.* **2017**, *51*, 2226–2234.
(39) Wu, C. M.; Baltrusaitis, J.; Gillan, E. G.; Grassian, V. H. Sulfur Dioxide Adsorption on ZnO Nanoparticles and Nanorods. *J. Phys. Chem. C* **2011**, *115*, 10164–10172.
(40) Vasile, B. S.; Oprea, O.; Voicu, G.; Ficai, A.; Andronescu, E.; Teodorescu, A.; Holban, A. Synthesis and Characterization of a Novel Controlled Release Zinc Oxide/Gentamicin-Chitosan Composite with Potential Applications in Wounds Care. *Int. J. Pharm.* **2014**, *463*, 161–169.
(41) Tavares, D. S.; Rodrigues, S. M.; Cruz, N.; Carvalho, C.; Teixeira, T.; Carvalho, L.; Duarte, A. C.; Trindade, T.; Pereira, E.; Römkens, P. F. A. M. Soil-Pore Water Distribution of Silver and Gold Engineered Nanoparticles in Undisturbed Soils under Unsaturated Conditions. *Chemosphere* **2015,** *136*, 86-94.
(42) Hoagland, D. R.; Arnon, D. I. *The Water-Culture Method for Growing Plants without Soil*, 2nd Edition.; Circ. Calif. Agric. Exp. Stn, **1950**.
(43) Gao, X.; Avellan, A.; Laughton, S.; Vaidya, R.; Rodrigues, S. M.; Casman, E. A.; Lowry, G. V. CuO Nanoparticle Dissolution and Toxicity to Wheat (Triticum Aestivum) in Rhizosphere Soil. *Environ. Sci. Technol.* **2018**, *52*, 2888–2897.
(44) Tso, C. P.; Zhung, C. M.; Shih, Y. H.; Tseng, Y. M.; Wu, S. C.; Doong, R. A. Stability of Metal Oxide Nanoparticles in Aqueous Solutions. *Water Sci. Technol.* **2010**, *61*,127-133.
(45) Ma, J.; Sun, Z.; Wang, Z.; Zhou, X. Preparation of ZnO–Cellulose Nanocomposites by Different Cellulose Solution Systems with a Colloid Mill. *Cellulose* **2016**, *23*, 3703–3715.
(46) John, A.; Ko, H. U.; Kim, D. G.; Kim, J. Preparation of Cellulose-ZnO Hybrid Films by a Wet Chemical Method and Their Characterization. *Cellulose* **2011**, *18*, 675–680.
(47) Ye, S.; Zhang, D.; Liu, H.; Zhou, J. ZnO Nanocrystallites/Cellulose Hybrid Nanofibers Fabricated by Electrospinning and Solvothermal Techniques and Their Photocatalytic Activity. *J. Appl. Polym. Sci.* **2011**, *121*, 1757–1764.
(48) Corradini, E.; de Moura, M. R.; Mattoso, L. H. C. A Preliminary Study of the Incorparation of NPK Fertilizer into Chitosan Nanoparticles. *Express Polym. Lett.* **2010**, *4*, 509–515.
(49) Regiel-Futyra, A.; Kus-Liśkiewicz, M.; Wojtyła, S.; Stochel, G.; Macyk, W. The Quenching Effect of Chitosan Crosslinking on ZnO Nanoparticles Photocatalytic Activity. *RSC Adv.* **2015**, *5*, 80089–80097.
(50) Waalewijn-Kool, P. L.; Diez Ortiz, M.; Van Straalen, N. M.; Van Gestel, C. A. M. Sorption, Dissolution and PH Determine the Long-Term Equilibration and Toxicity of Coated and Uncoated ZnO Nanoparticles in Soil. *Environ. Pollut.* **2013**, *178*, 59–64..
(51) Donner, E.; Broos, K.; Heemsbergen, D.; Warne, M. S. J.; McLaughlin, M. J.; Hodson, M. E.; Nortcliff, S. Biological and Chemical Assessments of Zinc Ageing in Field Soils. *Environ. Pollut.* **2010**, *158*, 339–345.
(52) Romero-Freire, A.; Lofts, S.; Martín Peinado, F. J.; van Gestel, C. A. M. Effects of

Aging and Soil Properties on Zinc Oxide Nanoparticle Availability and Its Ecotoxicological Effects to the Earthworm Eisenia Andrei. *Environ. Toxicol. Chem.* **2017**, *36*, 137–146.

(53) Ma, W. C.; Bonten, L. T. C. Bioavailability Pathways Underlying Zinc-Induced Avoidance Behavior and Reproduction Toxicity in Lumbricus Rubellus Earthworms. *Ecotoxicol. Environ. Saf.* **2011**, *74*, 1721–1726.

(54) Kanakaraju, D.; Ravichandar, S.; Lim, Y. C. Combined Effects of Adsorption and Photocatalysis by Hybrid TiO2/ZnO-Calcium Alginate Beads for the Removal of Copper. *J. Environ. Sci. (China)* **2017**, *55*, 214–223.

(55) Marschner, H. Zinc Uptake from Soils. In *Zinc in Soils and Plants*; Robson A.D., Ed.; Springer, Dordrecht.**1993**

(56) Hortin, J. M.; Anderson, A. J.; Britt, D. W.; Jacobson, A. R.; McLean, J. E. Soil-Derived Fulvic Acid and Root Exudates, Modified by Soil Bacteria, Alter CuO Nanoparticle-Induced Root Stunting of Wheat: Via Cu Complexation. *Environ. Sci.: Nano* **2019**, *6*, 3638–3652.

(57) Gao, X.; Rodrigues, S. M.; Spielman-Sun, E.; Lopes, S. ; Rodrigues, S.; Zhang, Y.; Avellan, A.; MBO Duarte, R.; Duarte, A.; Casman, E. A.; et al. Effect of Soil Organic Matter, Soil PH, and Moisture Content on Solubility and Dissolution Rate of CuO NPs in Soil. *Environ. Sci. Technol.* **2019**, *53*, 4959-4967.

For Table of Contents Only